Nonlinear modelling and analysis of an AMB system in the harmonic domain*

J. Jugo, I. Lizarraga, I. Arredondo
Electricity and Electronics Department
University of the Basque Country, Spain.
josu@we.lc.ehu.es

***Abstract*— In this work, the nonlinear modelling and analysis of an AMB system, based on the *MBC500 Rotor Dynamics* from Launchpoint Technologies, is presented. This approach is based on the harmonic domain linearization of the AMB system around a nonlinear stationary solution, under different rotating speeds. The nonlinear nature of the response appears at high speeds, due to the large oscillations introduced by the shaft unbalance. Using the presented methodology, low frequency gain loss is detected when increasing the rotating speed. This phenomenon causes the instability of the system, leading to destructive crashes.**

***Index Terms*— AMB system, rotor dynamics, nonlinear analysis.**

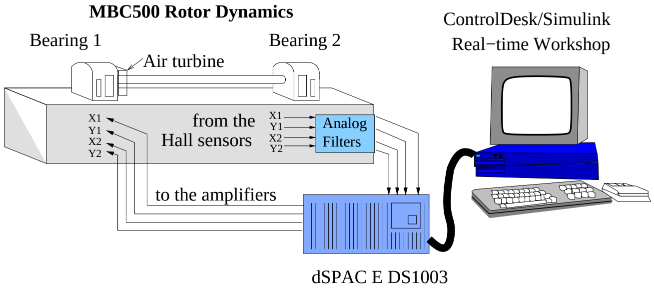

Fig. 1. Laboratory AMB system scheme

I. Introduction

Active magnetic bearings (AMB) are considered a serious design alternative in mechatronic systems because they provide remarkable advantages over conventional bearings. First, magnetic suspension requires no lubrication, making possible very high rotational speeds with longer life for the mechanical components. Second, magnetic bearings can be used as actuators for making an active control of the shaft [8]. However, this technology needs a control loop to stabilize the plant, and the resulting nonlinear dynamics introduced by the magnetic forces leads to sub-damped responses. Hence, the analysis of these features is fundamental for obtaining an adequate behaviour. Consequently, in the past, much work has been carried out on the subject of nonlinear modelling, stability and bifurcation analysis of this class of systems, [3], [4], [9] and in the design of linearization procedures, [12].

On the other hand, harmonic domain techniques are currently used for the analysis of nonlinear systems in several engineering areas, [5], [2]. In this work, the nonlinear modelling and analysis in the harmonic domain of a laboratory AMB system based on the *MBC500 Rotor Dynamics* from Launchpoint Technologies [10], extending the linearization method proposed in [5], is presented. The modelling is performed obtaining the evolution of the LTV models calculated around different rotating speeds. The nonlinear analysis of the resulting system shows the presence of a bifurcation point leading to instability around 400 Hz rotating speed. In addition, the harmonic analysis of the nonlinearity shows the low frequency gain loss as the rotating speed is increased. This gain loss which is specially noted starting at 300 Hz, explains the instability observed, and this effect appears in the vicinity of a mechanical resonance corresponding to a flexible mode of the shaft.

In Section 2, the AMB system description and modellization process is presented. In Section 3, the harmonic domain nonlinear analysis of the AMB system is carried out from a theoretical and a numerical point of view. In addition, the experimental results presented in Section 4 validate the proposed analysis and the conclusions end the paper.

II. AMB system description

The laboratory device which has been used as testbed for the proposed methodology is composed by an AMB system (i.e., the plant under study), a DSP based controller and a PC supervisor used for programming and monitoring purposes, Fig. 1. The plant is the *MBC500 Rotor Dynamics* which has been specially designed for academical purposes and it is composed of two AMBs and a rotor which includes an air turbine drive, allowing speeds up to 22000 rpm. The shaft position is measured by Hall effect sensors and the currents causing the forces in the bearings to maintain the hovering state, are driven by voltage amplifiers. Thus, the plant inputs are the voltages given to the amplifiers from the DSP controller, and the outputs are the voltages provided by the Hall-effect sensors and filtered, in order to minimize the noise at high frequencies. Those filtered measurements are the input signals for the controller, which has been designed for stabilizing the closed loop dynamics, [1], [6].

The modelling can be performed following different ways, [1]. In this case, the analysis has been carried out per-

* The authors are very grateful to the CICYT, the university of the Basque Country and the Basque Government for the partial support of this work, through projects DPI2002-04155-C02-01, PTR95-0897.OP.CT and 9/UPV00224.310-15254/2003, and the Predoctoral grant BF104.466, respectively.

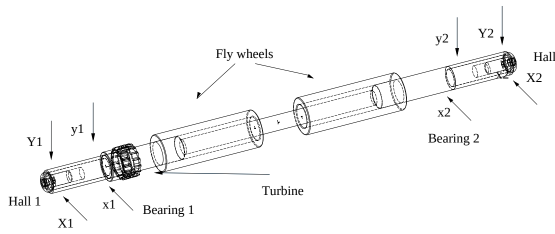

Fig. 2. Detailed mechanical structure of the rotor showing FEA points

forming a complete *Finite Element Analysis* (FEA) analysis, starting from the CAD description of the shaft facilitated by the device producer, Launchpoint Technologies [10].

A. Model of the mechanical subsystem

The mechanical part of the system is composed basically by the shaft, where the magnetic forces F_{x_1}, F_{x_2}, $F_{y_1}$and F_{y_2} generated by the bearings at distance l in the x and y directions are considered the inputs , and the motion generated at the bearings positions and the positions of the Hall effect sensors, denoted by the variables $\{x_1,\ x_2,\ y_1,\ y_2\}$ and $\{X_1,\ X_2,\ Y_1,\ Y_2\}$, respectively, are the outputs (see Fig. 2). The model, described by system equations (1), includes the effects of the shaft flexibilities and has been obtained by a FEA analisys using the Structural Dynamics Toolbox of SDTools, starting from the mesh of the original CAD description in SolidWorks, and considering the rigid body modes and the first and the second elastic modes of the shaft in the x and y directions.

$$\begin{aligned} [\dot{x}_{shaft}] &= A_{shaft}\,[x_{shaft}] + B_{shaft}\,[F_{mag}] \qquad (1) \\ \begin{bmatrix} P_{hall} \\ P_{bearing} \end{bmatrix} &= [C_{shaft}]\,[x_{shaft}] = [C_{rig},\, C_{flex}]\,[x_{shaft}] \end{aligned}$$

where $F_{mag} = (F_{x_1}, F_{y_1}, F_{x_2}, F_{y_2})^T$ are the magnetic forces, $P_{hall} = (X_1, Y_1, X_2, Y_2)^T$ the shaft position in the Hall sensors and $P_{bearing} = (x_1, y_1, x_2, y_2)^T$the shaft position in the bearings[1].

In addition, other effects are:

1. Gravity effect: The gravity (g) is introduced as an external force in order to maintain the same model for the x and y axis, leading to augment the input matrix with another term B_{weight} (see footnote 1). The gravity supposes a bended beam in the y axis direction, even in static position, due to the shaft flexibilities.

2. Rotating unbalance model: Different factors such as imperfections on the rotor can produce the unbalancing. When $\omega \neq 0$, this unbalance introduces a centrifugal force F_{ctf_i} which is proportional to the square of the rotating velocity ω.

3. Gyroscopic effect: The shaft length and width lead to neglect its influence in the work frequency range, [7].

The modelling of the unbalance has been performed introducing external forces at different points of the shaft, in order to simulate the effect of the centrifugal forces.

$$\begin{bmatrix} F_{ctf_1} \\ F_{ctf_2} \end{bmatrix} = \omega^2 \begin{bmatrix} sin\omega t \\ cos\omega t \end{bmatrix} \qquad (2)$$

[1]The system matrices A_{shaft}, B_{shaft}, C_{shaft}, B_{rot} and B_{weight} are accessible in the web, http:/www.ehu.es/gaudee/jjugo/matrices.html

Those forces have been considered using the Structural Dynamics toolbox and selecting the values of the gains affecting each external force at different points exciting translational and conical modes in order to get a similar behaviour for simulated and experimental results. Thus, a new term B_{rot} (see footnote 1) must be included in the input matrix.

Thus, the mechanical model is obtained linking those effects, being the inputs to the system the forces in the bearings, the centrifugal forces (2) and the gravity and being the outputs the positions measured at the location of the Hall sensors and bearings. So, the total input matrix B_{total} results

$$B_{total} = [B_{shaft},\, B_{rot},\, B_{weight}]$$

and the input forces are $F_{total} = (F_{x_1} + 0.5F_{ctf_1}, F_{y_1} + 0.5F_{ctf_2}, F_{x_2} - 0.5F_{ctf_1}, F_{y_2} - 0.5F_{ctf_2}, F_{ctf_1}, F_{ctf_2}, F_{ctf_1}, F_{ctf_2}, Mg)^T$.

B. Model of the other elements

To complete the model of the laboratory device, it is necessary to include now the rest of elements present in the scheme of the figure 1: the forces provided by the electromagnetic bearings, the dynamics of the amplifiers, sensors and filters and, finally, the controller.

Magnetic forces: Due to the differential mode configuration of the bearings, the electromagnetic forces can be written as:

$$\begin{aligned} F_{x_i} &= K\frac{(i_{x_i}+i_0)^2}{(x_i-x_g)^2} - K\frac{(i_{x_i}-i_0)^2}{(x_i+x_g)^2} \quad i=1,2 \qquad (3) \\ F_{y_i} &= K\frac{(i_{y_i}+i_0+i_c)^2}{(y_i-y_g)^2} - K\frac{(i_{y_i}-i_0+i_c)^2}{(y_i+y_g)^2}, \quad i=1,2 \end{aligned}$$

where $K = 2.8 \times 10^{-7} N \cdot m^2/A^2$ is a geometric constant depending on the bearing, $i_0 = 0.5$A is a bias current, $x_g = y_g = 0.0004m$ is the mean distance between the bearing and the rotor and i_{x_i} and i_{y_i}, $i = 1, 2$, are the currents in the two bearings for the x and y directions, respectively. In the y direction, an unbalanced current bias with $i_c = 0.2\,A$ has been introduced in order to compensate the effect of the gravity.

Amplifier's dynamics: The amplifier's dynamics has been supplied by the device producer, [10], and it is given by:

$$i_i = \frac{0.25}{(1+2.2\times10^{-4}s)} A/V \times V_{control_i}, \quad i=1,2 \qquad (4)$$

in both, x and y, directions, that is, for $i_{x_i}$and i_{y_i}.

Hall sensors: The linearized sensors' response has been supplied by the device producer and it is described by (5):

$$V_{sensor_i} = 10V/mmX_i \pm 1V\,offset, \quad i=1,2 \qquad (5)$$

in both, x and y, directions.

Filters's dynamics : Noise reduction filters have been developed and introduced for filtering the Hall sensors's measurements, being the model given by Equation (6).

$$V_{filt_i} = \frac{4000}{s+4000} V_{sensor_i}, \quad i=1,2 \qquad (6)$$

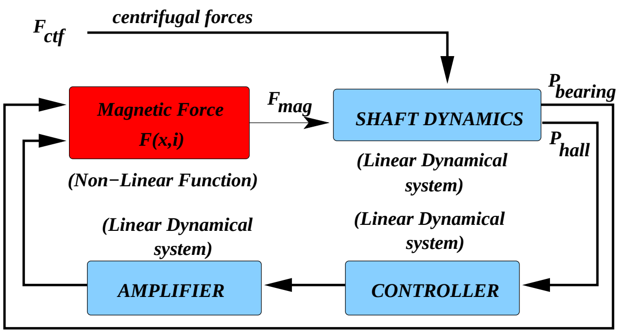

Fig. 3. Block-diagram of the AMB system

Controller design: After the modelling process, linearizing around an operating point and exploiting the symmetry in the resulting matrix function, the design of stabilizing controllers is possible, [6]. In this case two different stabilizing controllers are considered, a PD and a PID controller, using as input the filtered measurement in the sensors V_{filtr} and driving the ouput signal to the control voltages $V_{control}$. Considering the digital version of the controllers implemented in the actual DSP, those are given by the following discrete transfer functions:

$$PD(z) = \frac{7.5(z-0.5)}{z} \qquad T = 1e-4\,s \tag{7}$$

$$PID(z) = \frac{7.5(z-0.5)}{z}\,\frac{0.6006(z-0.998)}{z-1} \tag{8}$$

The related continuous versions used for analysis purposes are described by:

$$PD(s) = \frac{14.25s+15000}{s+20000} \tag{9}$$

$$PID(s) = \frac{14.25s+15000}{s+20000}\,\frac{12(s/20+1)}{s} \tag{10}$$

Then, the AMB system represented in Fig. 1 can be described by linking the shaft model (1), including rigid, flexible and unbalanced motion effects, and magnetic forces (3), sensor (5), filters (6) , amplifiers dynamics (4) and controllers (9) and (10). This model is shown esquematically in figure 3.

This model has been tested both in Scilab and Matlab/Simulink environments, [1], [6], with satisfactory results comparing with experimental measurements.

III. Nonlinear Analysis of the AMB System in the Harmonic Domain

Here, the theoretical basis for the nonlinear analysis are briefly introduced and then, they are applied to the rotor-AMB system. This analysis is based in the fact that the linearization of a nonlinear system around a periodic solution yields to a periodic linear time-varying system (PLTV). Applying the Floquet theorem, the stability of the periodic solution can be determined by computing the Floquet exponents or multipliers of the resulting PLTV system. In this work, this procedure is carried out in the harmonic domain.

For the sack of simplicity, a SISO nonlinear system described by the following state-space equations is considered:

$$\dot{x} = f(x, u_0, t) \tag{11}$$

Here $x(t)$ is the state vector, $u_0(t)$ the external source and $f(x, u_0, t)$ is a nonlinear function. Considering a periodic solution $x_0(t)$ of (11) with period T, the linearization of the system dynamics around the periodic solution, given a small-signal perturbation $\zeta(t)$, can be represented by the following LTV system:

$$\begin{aligned} \dot{\zeta}(t) &= G(t)\zeta(t) + B\ u(t) \\ y(t) &= C\zeta(t) \end{aligned} \tag{12}$$

where $G(t) = [Jf(x_0(t))]$ is the jacobian matrix evaluated along the periodic solution $x_0(t)$. A small-signal input vector $u(t)$ and linear combination of the state variables $y(t)$ has been considered for obtaining an input-output representation of the linearized system. The resulting matrices B and C are constant matrices of appropriate dimensions and $G(t)$ is periodic with the same period T, so system equations (12) represent a PLTV system.

Considering exponentially modulated periodic (EMP) signals as system input, [11], [13], $u(t) = \sum_{n\in\mathbb{Z}} U_n e^{s_n t}$, with $t \geq 0$, $s_n = s + jn\omega_0$, and $s \in C$, the steady-state response of the PLTV system (12) is also an EMP signal, being $\zeta(t) = \sum_{n\in\mathbb{Z}} Z_n e^{s_n t}$ and $y(t) = \sum_{n\in\mathbb{Z}} Y_n e^{s_n t}$.

Now, expanding the system matrix $G(t)$ as a Fourier series $G(t) = \sum_{k\in\mathbb{Z}} G_k e^{jk\omega_0 t}$ and introducing the series expansions above in the system equation (12) and equating the harmonic coefficients, the system can be expressed by mean of an infinite dimensional matrix equation:

$$\begin{aligned} sZ &= (Toeplitz(G) - \mathbf{N})\,Z + \mathbf{B}U \\ Y &= \mathbf{C}Z \end{aligned} \tag{13}$$

where the state $Z = [\ldots,\ Z_{-1},\ Z_0,\ Z_{+1}, \ldots]^T$, input signal $U = [\ldots,\ U_{-1},\ U_0,\ U_{+1}, \ldots]^T$ and output signal $Y = [\ldots,\ Y_{-1},\ Y_0,\ Y_{+1}, \ldots]$ are double infinite vectors and **N**, **B** and **C** are infinite dimensional block diagonal matrices. The diagonal elements in **B** and **C** are infinite instances of the input matrix B and output matrix C respectively and **N** is given by:

$$\mathbf{N} = diag\,\{jn\omega_0 I\} \quad n \in \mathbb{Z} \tag{14}$$

being I the identity matrix. Finally, *Toeplitz(G)* represents the double infinite Toeplitz matrix formed with the harmonic components of G:

$$toeplitz(G) = \begin{bmatrix} \ddots & \vdots & \vdots & \vdots & \vdots & \vdots & \iddots \\ \cdots & G_1 & G_0 & G_{-1} & G_{-2} & G_{-3} & \cdots \\ \cdots & G_2 & G_1 & G_0 & G_{-1} & G_{-2} & \cdots \\ \cdots & G_3 & G_2 & G_1 & G_0 & G_{-1} & \cdots \\ \iddots & \vdots & \vdots & \vdots & \vdots & \vdots & \ddots \end{bmatrix} \tag{15}$$

The stability of the PLTV system (12) is determined through the roots of the system matrix of (13), which are infinite eigenvalues of the type: $\lambda_i \pm jk\omega_0 \quad i = 1 \ldots n,\ k =$

$-\infty, \ldots, \infty$. These eigenvalues are the Floquet exponents of the LTV system (12) and the corresponding Floquet multipliers are $m_i = e^{(\lambda_i \pm jk\omega_0)T} \quad i = 1 \ldots n$.

For stability, Floquet multipliers should be locate inside the unit circle, or equivalently, the Floquet exponents should lie in the open left-hand plane. The evolution of the exponents or multipliers when varying a parameter gives the bifurcation locus of the system.

Now the previous analysis is applied to the rotor-AMB system using the model presented in section (II). Obviously, the stability analysis requires the previous calculation of the nonlinear periodic solution for each rotation velocity, which can be obtained by any numerical approach in the time domain or in the harmonic domain. The advantage in the harmonic domain is the possibility of obtain unstable solutions, interesting for analysis purposes.

In closed loop, as it is shown in Figure 3, the only external inputs to the system are the centrifugal forces for a particular rotating speed, which determine the periodic equilibrium point. System dynamics around this periodic solution depend on the shaft dynamics, on the controller and amplifier and on the magnetic force expression. In particular, the nonlinear behaviour of the system is only due to the magnetic force acting in the AMBs . The modelization process, in order to obtain the harmonic equation (13), can be performed separating the nonlinear and linear parts, linearizing the nonlinear parts and combining the overall system as a linear system following the scheme of Figure 3. Note that the linear parts must be expanded to all the harmonic components according to (13)-(15).

Hence, as a first step in the stability analysis, the linearization of the nonlinear part of the system around a particular periodic solution is carried out. The resulting jacobian matrix $G_F(t)$ is the jacobian of the magnetic force and it is a time-dependent term that represents the nonlinear subsystem. The magnetic force acting in each bearing only depends on the current through this bearing and on the spatial variable that is controlled for the bearing, so the force jacobian can be written as:

$$G_F = \begin{bmatrix} \frac{\partial F_{x_1}}{\partial x_1} & 0 & 0 & 0 & \frac{\partial F_{x_1}}{\partial i_{x_1}} & 0 & 0 & 0 \\ 0 & \frac{\partial F_{x_2}}{\partial x_2} & 0 & 0 & 0 & \frac{\partial F_{x_2}}{\partial i_{x_2}} & 0 & 0 \\ 0 & 0 & \frac{\partial F_{y_1}}{\partial y_1} & 0 & 0 & 0 & \frac{\partial F_{y_1}}{\partial i_{y_1}} & 0 \\ 0 & 0 & 0 & \frac{\partial F_{y_2}}{\partial y_2} & 0 & 0 & 0 & \frac{\partial F_{y_2}}{\partial i_{y_2}} \end{bmatrix} \tag{16}$$

This jacobian can be obtained in the harmonic domain analitically from (3) by means of Taylor series and Fourier series expansion or following a numerical procedure as follows. Althout the exact description of the system needs of an infinity number of harmonics in the expansion, taking into account that the contribution of each harmonic decays when increasing the order, only a couple of harmonics are needed to be considered, depending on the nonlinearity grade, in order to obtain an accurate approximation.

Considering the AMB system with static MISO nonlinearities $y = f(u_i)$, $i = 1, 2, \ldots, n$, the numerical way for obtaining the harmonic components of the jacobian (16) is described in the scheme of figure 4. Starting from a periodic equilibrium solution for the system under study, the inputs $u_i \ i = 1, 2, \ldots, n$, must be described in the time-domain and the partial derivatives of f respect the inputs must be calculated. Concretely, for the nonlinear magnetic forces, the inputs are the bearing currents and the position. The resulting signals representing the partial derivatives of the forces around the periodic steady state are mathematically described by a finite number of points along a period and those can be transformed to the harmonic domain using *fft* functions, obtaining the precised coefficients for the jacobian (16), in a similar way to the partial derivatives for an analitical approach.

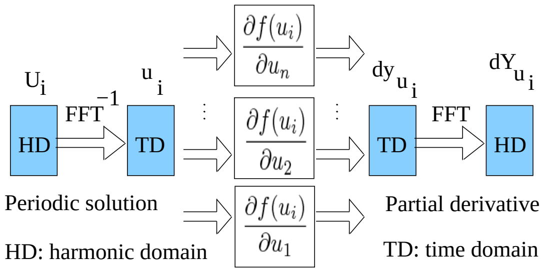

Fig. 4. Numerical obtaining of Fourier coefficients for the linearization process

The harmonic expansion for the global system matrix $G(t)$ (13) results from combining the force jacobian representing the nonlinear subsystems with the linear terms as stated above, following the scheme of figure 3. Now, the constant (but complex) harmonic state space equation (13) can be written and the stability of the periodical solution can be easily analyzed through the computation using matrix based algorithms of the Floquet exponents, i.e., the system eigenvalues, which are periodic with same period as the solution under study.

Applying this procedure to the AMB system described in section II, PLTV models describing the behaviour of the system at different rotating speed can be obtained. However, due to the high order of the obtained state-space equations, even using only the two first harmonics of the expansion (72 state variables), the overall PLTV models are not shown in this work. In addition, the system behaviour is analyzed by mean of an unique Floquet exponent. This Floquet exponent obtained for different rotating speeds resumes the stability information.

Numerical results

Two different cases are considered, corresponding to the use of the PD and PID controllers, (9) and (10), respectively. In both cases, the analysis of the obtained periodic LTV models shows how a Floquet exponent suddenly leads toward instability for rotating speeds up to 400Hz (which is similar to the experimentally obtained result). As can be observed in Fig. 5, PD case, a spurious oscillation is predicted near to 50 Hz (this fact is also experimentally

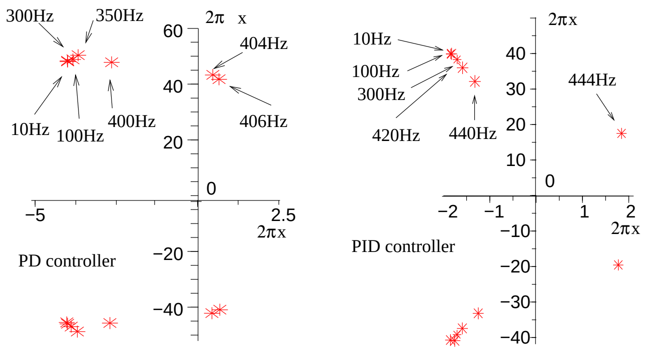

Fig. 5. Evolution of the system Floquet exponent with respect to different rotating speeds. A Hopf bifurcation point near 400Hz rotating speed is detected.

observed), that is, the system presents a Hopf bifurcation point depending of the rotating speed.[2]. In PID case, the nonlinear effects leading a Hopf bifurcation appear at higher rotating speeds, around 450 Hz, when the centrifugal forces are more important, being the frequency of the predicted oscillation around 30 Hz.

In order to explain this nonlinear effect, the continuous component of the magnetic force has been studied at different rotating speeds. In Fig. 6, the evolution of the magnetic force continuous gain in the two bearings (x and y directions) with respect to the current i shows a gain loss, which is remarkable in one of the bearings near the rotating speed of 400 Hz and 450 Hz. That is, the nonlinear magnetic force leads to a low frequency gain loss which causes the system instability at high rotating speeds. In fact, the influence of the harmonics introduced by the nonlinearity reinforces this effect.

The form of the magnetic force respect to the coil current parametrized respect to the distance of the shaft from the origin, and the superposed actual evolution of this magnetic force at different rotating speed is represented in Figure 7. Observing this form, it can be concluded that the nonlinearity is more relevant when increasing the distance of the shaft from the origin. Then, since increasing the rotating speed the centrifugal force caused by the unbalance is higher, at higher speeds the curve traveled through the force surface in the nonlinear zone is more relevant. The result is the relative gain loss.

In fact, the PD controller try to compensate this loss in order to maintain stability, distancing the shaft from the origin in the sensor position and, hence, increasing the importance of the nonlinearity since this system is almost collocated. On the other hand, the PID controller compensates the necessity of move the shaft from the origin for compensating the gain loss and, for this reason, the obtained result is better.

[2]Remember that the centrifugal forces depend on the rotating speed as $f_{ctf} \sim \omega^2$

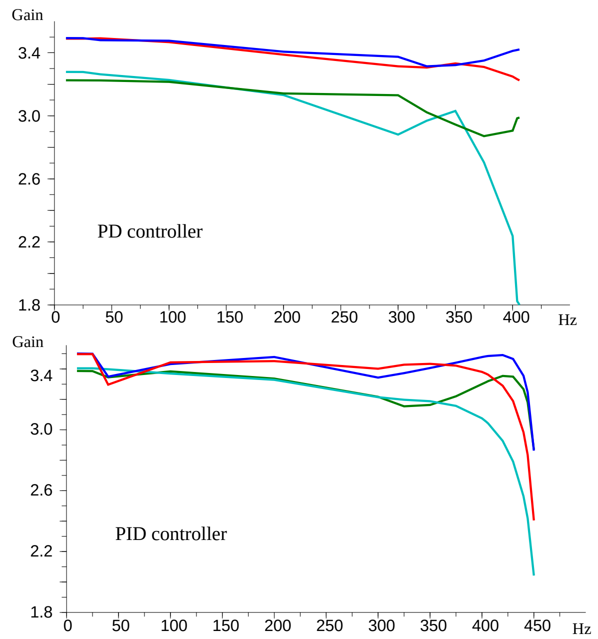

Fig. 6. Continuous component of the four magnetic forces (x and y axis, in the two bearings) respect to the current i using both PD and PID controller

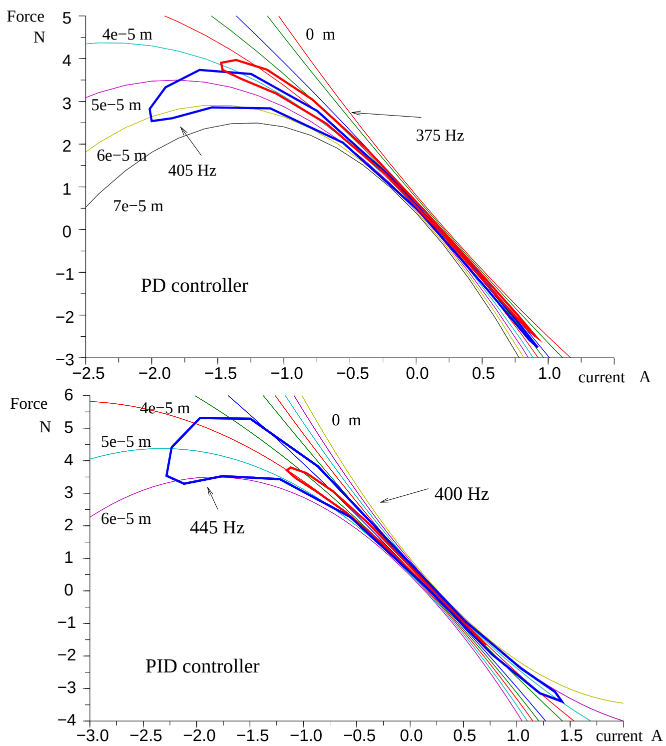

Fig. 7. Magnetic force respect to the current at different distances from the origin and actual behaviour at two different rotating speeds

In any case, note that the stability problems appear when the rotation behaviour gives very distorted signals, that is, when appearing harmonics components with large level. Actually, the unstable behaviour presented by the AMB system is directly related to the mechanical resonance due to the second flexible mode of the shaft, around 450 Hz, [1]. The bearings are not able to give the necessary force to compensate the mentioned resonance. As is observed in figure 7, the magnetic force is limited by its nonlinear nature.

IV. Experimental results

As has been stated in the section II, the modeled system is a laboratory testbed which scheme is shown in figure 1. Implementing the digital versions of the controllers used in the theoretical analysis, equations (7) and (8), the same qualitative results are obtained. The main difference between actual and theoretical ones is a light reduction of the stability range in the experimental device, since the actual frequency resonance of the device is lower and the digital versions of the controllers add a time-delay to the feedback system. Hence, when in the simulated model the stability range is around 400 Hz for the PD and 450 Hz for the PID in the real case this range is reduced in more that a 10%, as can be observed in the figure 8.

However, validating the analysis performed in the previous section, the instability theoretically predicted around 50 Hz appears in the experimental testbed (PD controller). That is, the analysis technique has been successfully applied to a complex system, the AMB system, explaining its nonlinear regimen.

V. Conclusions

In this paper, the harmonic domain (HD) modelling and analysis of an AMB system, based on the *MBC500 Rotor Dynamics*, is presented. This HD analysis technique allows the obtaining of LTV models around nonlinear periodic solutions. In this case, those models give the possibility to analyze the AMB system at different rotating speeds, showing a Hopf bifurcation point. In addition, the analysis shows that this nonlinear effect is due to a low frequency gain loss which appears when the shaft is rotating at speed leading to large signal distortions. This approach has been carried out with PD and PID controllers, obtaining similar conclusions and agreeing the experimental and numerical results.

Those results enforce the idea that linearization techniques for the magnetic force or techniques limiting the work zone around the origin of the shaft are the more suitable methods in order to improve the behaviour of AMB systems.

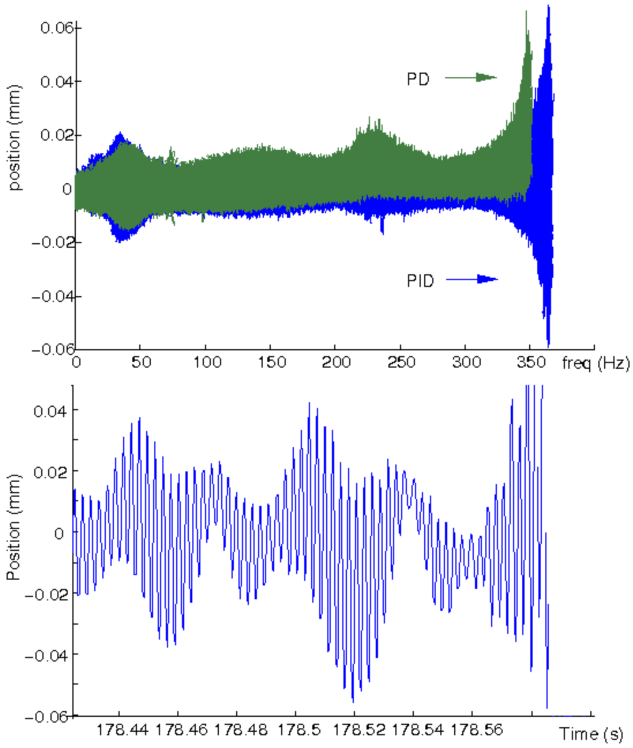

Fig. 8. Up: Rotating speed depending stability range using the PD and PID controller. Down: Nonlinear oscillation range using the PD controller in the x_{hall} position.

References

[1] I. Arredondo, J. Jugo and V. Etxebarria, Modelling of a flexible rotor AMB system, ACC American control conference, *accepted*, Minneapolis, USA, 2006.

[2] S. Banerjee and .C Verghese, Nonlinear phenomena in power electronics, IEEE Press, 2001.

[3] J.C. Ji, L. Yu and A.Y.T. Leung, Bifurcation behaviour of a rotor supported by active magnetic bearings, J. of Sound and Vibration, vol. 235(1), pp. 133-151, 2000.

[4] J.C. Ji, Stability and Hopf bifurcation of a magnetic bearing system with point delays, J. of Sound and Vibration, vol. 259(4), pp. 845-856, 2003.

[5] J. Jugo, A. Anakabe and J.M. Collantes, Control design in the harmonic domain for microwave and RF circuits, IEE Proc. Control Theory and Applications, vol. 150(2), pp. 127-131, 2003.

[6] J. Jugo, I. Arredondo, Analysis and control design of MIMO systems based on symmetry properties, CDC-ECC'05, Seville, Spain, 2005.

[7] C. Lee, Vibration Analysis of Rotors, Kluwer academic, Dordrecht, 1993.

[8] G. Schweitzer, H. Bleuler, and A. Traxler, *Active Magnetic Bearings: Basics, Properties and Applications of Active Magnetic Bearings.* vdf Hochschulverlag AG an der ETH Zurich, 1994.

[9] N. Steinschaden and H. Springer, Nonlinear stability analysis of active magnetic bearings, Proceedings of ISMB 5, California, USA, 1999.

[10] (2005) The LaunchPoint website. [Online]. Available: http://www.launchpnt.com/

[11] N. M. Wereley and S. R. Hall, Frequency response of linear time periodic systems, Proc. of the 29th IEEE Conference on Decision and Control, Honolulu, Hawaii, pp. 3650-3655, 1990.

[12] H. Yasoshima, M. Kawanishi, H. Kannki, Application exact linearization to AMB system, Proceedings of the 8^{th} International Symposium on Magnetic Bearings, 2002.

[13] J. Zhou, T. Hagiwara and M. Araki, Stability analysis of continuous-time periodic systems via the harmonic analysis, IEEE Transaction on Automatic control, vol. 47(2), pp. 292-298, 2002.